Ion-size effect on superconducting transition temperature T_c in $R_{1-x-y}Pr_xCa_yBa_2Cu_3O_{7-z}$ systems (R=Er, Dy, Gd, Eu, Sm, and Nd)

Li-Chun Tung, J. C. Chen, M. K. Wu, and Weiyan Guan
Department of Physics, National Tsing Hua University, Hsinchu, 300, Taiwan, Republic of China
(Received 14 September 1998)

We observed a rare-earth ion-size effect on T_c in $R_{1-x-y}Pr_xCa_yBa_2Cu_3O_{7-z}$ (R=Er, Dy, Gd, Eu, Sm, and Nd) systems which is similar to that in $R_{1-x}Pr_xBa_2Cu_3O_{7-z}$ systems in our previous reports. For fixed Pr and Ca concentration (fixed x and y), T_c is linearly dependent on rare-earth ion radius r_R^{3+}. For a fixed Pr concentration x, there exists a maximum of T_c ($T_{c,\max}$) in T_c vs Ca concentration y curves. $T_{c,\max}$ shifts to higher Ca concentration region for samples with larger R ion radius. The enhancement of T_c ($\Delta T_{c,\max}=T_{c,\max}-T_{c,y=0}$; $T_{c,y=0}$ is the transition temperature T_c without Ca doping) increases with increasing R ion radius. We proposed an empirical formula for T_c (r_R^{3+},x,y) to fit our experimental data: $T_c(x,y)=T_{c0}-A\beta^2(\alpha/x+y/\beta)^2-Bx$. All fitting parameters in this formula, T_{c0}, B, β, α/β, and $A\beta^2$, are rare-earth ion-size dependent. [S0163-1829(99)01506-4]

I. INTRODUCTION

The substitution of Y by trivalent rare-earth elements in orthorhombic $YBa_2Cu_3O_{7-y}$ (YBCO), yields a superconducting phase with T_c identical to YBCO,[1] except for Ce, Tb, Pm, and Pr. It shows that the magnetic moments of the lanthanide ions have a weak effect on the CuO_2 sheets. The insensitivity of the superconducting properties to the substitution is presumably due to their layered structure and the nearly complete lack of interaction between rare-earth and CuO_2 sheets.[2]

Although crystallographically identical to all the other rare-earth-based superconductors, $PrBa_2Cu_3O_{7-y}$ (PrBCO) inhibits the superconducting and metallic behavior.[3–5] The $Y_{1-x}Pr_xBa_2Cu_3O_{7-y}$ system is particularly interesting since it is isostructural to YBCO, yet the superconductivity is strongly suppressed as a function of Pr concentration.

The suppression of T_c by Pr doping in $Y_{1-x}Pr_xBa_2Cu_3O_{7-y}$ has been attributed to several possible mechanisms. The first mechanism involves the filling of holes (hole filling) in CuO_2 sheets due to the substitution of Pr ions with its valence greater than +3 and, hence, implies the suppression of superconductivity and metallic behavior, arising from a reduced number of carriers (holes) in CuO_2 sheets. Indeed, magnetic susceptibility,[4–6] Hall measurements,[5] thermoelectric power,[7] muon spin resonance,[8] neutron diffraction,[9] specific-heat measurement,[10] and x-ray-absorption spectroscopy[11] are consistent with a Pr valence substantially larger than 3+. Superconductivity observed in a $Pr_{0.5}Ca_{0.5}Ba_2Cu_3O_{7-y}$ film[12] strongly supports this mechanism. Based on the spin-polaron model, Wood[13] obtained an agreement with experimental data for a Pr concentration dependence of T_c in the $Y_{1-x}Pr_xBa_2Cu_3O_{7-y}$ system.

However, this idea was later questioned. X-ray-absorption near-edge spectroscopy,[14] valence-band resonant photoemission,[15] lattice constant[16] and Raman spectrum[17] indicate a Pr valence close to 3+. According to electron-energy-loss spectroscopy measurement,[18] the total number of holes on O sites was shown to be independent of Pr concentration x. It suggests that Pr ions are trivalent and localize, rather than fill, the mobile holes on CuO_2 planes. The localization leads to the suppression of superconductivity and induces a metal-insulator transition. In fact, most experimental results supporting hole filling would also support hole localization. Recently, Kao, Yu, and Guan[19] measured the hole concentration p per unit cell by using iodometric titration technique for $(Gd_{1-x}Pr_x)Ba_2Cu_3O_{7-y}$ ($x=0.1-0.9$) and $(R_{0.8}Pr_{0.2})Ba_2Cu_3O_{7-y}$ (R=Yb, Er, Dy, Gd, and Nd) samples. The chemical hole concentration p was compared to the Hall number $\mathbf{n}_H$ and T_c reported in literature. What is most surprising is that the total carrier concentration p is independent of Pr concentration and remains primarily constant even when the samples are not superconducting in higher Pr concentration region ($x\geqslant 0.5$) in $(Gd_{1-x}Pr_x)Ba_2Cu_3O_{7-y}$.[19] It should also be noted that the total carrier concentration p remains primarily constant even when T_c is changed by almost 100% with the changing of R ions in $(R_{0.8}Pr_{0.2})Ba_2Cu_3O_{7-y}$.[19] The authors proposed that the total hole concentration p measured by iodometric technique is not changed with Pr doping but the concentration of mobile holes $\mathbf{n}_H$ measured by the Hall effect is changed with T_c and Pr doping. It strongly suggests that T_c suppression appears to be caused by hole localization rather than hole filling.

The second mechanism for T_c suppression involves the spin-flip effect of the pairing electrons (pair breaking), being explained on the basis of Abrikosov-Gor'kov (AG) theory,[20] which has been used widely and successfully for interpretation of conventional alloy superconductors with paramagnetic doping. This model suggests Pr ion acts as a strong magnetic pair breaker.[6,21–23] AG theory predicts that a reduced transition temperature T_c/T_{c0} will be a universal function of the reduced concentration $x/x_{\rm cr}$,

$$\ln[T_c/T_{c0}]=\Psi(1/2)-\Psi(1/2+0.14xT_{c0}/x_{\rm cr}T_c), \quad (1)$$

where T_{c0} is the T_c for ''pure'' material (without doping), $x_{\rm cr}$ is the critical concentration for complete suppression of

superconductivity and Ψ is a digamma function. For $x \approx 0$, it gives an asymptotic form,

$$T_c = T_{c0} - [(\pi/4k_B)N(E_F)\tau^2(g-1)^2 J(J+1)]x, \quad (2)$$

where $N(E_F)$ is the density of state at Fermi level and g and J, respectively, the Landé g factor and the total angular momentum of Hund's rules ground state of the Pr ion and τ is the exchange interaction parameter.

The close correspondence of T_c vs x data with results based on AG theory [Eq. (2)] has been interpreted as an evidence for pair breaking.[21–23] Spin-polarized electronic band-structure calculations[24] for $R\mathrm{Ba_2Cu_3O_{7-y}}$ (R=Y, Gd, and Pr) also confirms the pair-breaking mechanism. AG theory (pair-breaking model) successfully explained the basic features of experiments, but the theory is difficult to explain the metal-insulator transition at larger Pr concentration in $(\mathrm{Y_{1-x}Pr_x})\mathrm{Ba_2Cu_3O_{7-y}}$.[3,4,6,21,25]

Fehrenbacher and Rice[26] proposed that the difference between $\mathrm{PrBa_2Cu_3O_{7-y}}$ and other $R\mathrm{Ba_2Cu_3O_{7-y}}$ comes from an enhanced stability of the $\mathrm{Pr^{IV}}$ state due to the hybridization with oxygen neighbors, involving the transfer of holes from primary planar O $2p\sigma$ to $2p\pi$ states. A particularly important unusual characteristic of Pr ions is its $4f$ wave function, while the other rare-earth ions are characterized by more symmetric orbital. Hybridization could generate an exchange interaction between the Pr magnetic moment and the mobile holes on $\mathrm{CuO_2}$ planes, leading to hole localization and/or pair breaking. Though this model has been widely used in discussion of $\mathrm{Y_{1-x}Pr_xBa_2Cu_3O_{7-y}}$, it could not explain the rare-earth ion-size effect on T_c in the $\mathrm{R_{1-x}Pr_xBa_2Cu_3O_{7-y}}$ system.[27,28]

After systematic studies of the superconducting and normal-state properties of the $\mathrm{R_{1-x}Pr_xBa_2Cu_3O_{7-y}}$ system, Guan and co-workers reported that the superconducting transition temperature T_c,[27] the magnetic ordering temperature of Pr ions T_N,[28] the normal-state resistivity ρ,[29,30] and the Hall number per unit cell $\mathbf{n}_H$ in $\mathrm{R_{1-x}Pr_xBa_2Cu_3O_{7-y}}$ (Ref. 30) are all R ion-size dependent. It was also reported that the Hall number $\mathbf{n}_H$ of $\mathrm{R_{0.9}Ca_{0.1}Ba_2Cu_3O_{7-y}}$ (Ref. 31) and T_c of $R\mathrm{Ba_2Cu_{3-x}Ga_xO_{7-y}}$ (Ref. 32) are also ion-size dependent.

For a constant Pr concentration, T_c of $\mathrm{R_{1-x}Pr_xBa_2Cu_3O_{7-y}}$ linearly decreases with increasing R ion radius, and the c-axis per unit cell increases with increasing R ion radius. One would expect the opposite trend based on the hybridization picture, since the average distance between $\mathrm{CuO_2}$ plane becomes larger leading to a weaker Pr-$\mathrm{CuO_2}$ hybridization. Khomdskii[33] suggested that Pr can induce a lattice distortion, especially the buckling of the $\mathrm{CuO_2}$ plane. It was established that the distance between Pr and its surrounding oxygen, $d_{\mathrm{Pr\text{-}O}}$, is less than $d_{\mathrm{Y\text{-}O}}$. If $d_{\mathrm{Pr\text{-}O}}$ keeps invariant in all $\mathrm{R_{1-x}Pr_xBa_2Cu_3O_{7-y}}$, one would expect a stronger buckling for $\mathrm{R_{1-x}Pr_xBa_2Cu_3O_{7-y}}$ with larger R ion radius, leading to larger resistivity and stronger suppression of superconductivity.

Among all cation dopiness, Ca substitution for Y in YBCO has attracted much attention.[34–40] The valence state of $\mathrm{Ca^{2+}}$ is lower than that of $\mathrm{Y^{3+}}$. Such a substitution will generate excess holes and T_c is suppressed by the overdoping effect. On the other hand, it has been known that Ca doping is likely to cointroduce oxygen vacancies, reducing the number of the generated holes. This indicates that doping with Ca ions has a counterbalance effect on the suppression of T_c.

Ca doping is able to increase the T_c of the oxygen-deficient YBCO.[35] The replacement of 20% Ca ions in tetragonal $\mathrm{YBa_2Cu_3O_6}$ induces the superconductivity; whereas the same amount of Ca, in fully oxygenated $\mathrm{YBa_2Cu_3O_{7-y}}$, lowers T_c from 90 to 78 K. Yakabe *et al.*[36] showed that there exists a maximum of T_c about 90 K with the variation of the carrier density in single phase $\mathrm{Y_{1-x}Ca_xBa_2Cu_3O_{7-y}}$ thin films up to 50% Ca concentration. Similar behavior was observed in $\mathrm{Y_{1-x}Ca_xBa_2Cu_{2.64}Co_{0.36}O_{7-y}}$,[37] $\mathrm{Y_{1-x}Ca_xBa_2Cu_{2.5}Fe_{0.5}O_7}$,[38] $\mathrm{Y_{1-x}Ca_xSr_2Cu_{3-y}M_yO_{6+z}}$ (M=Ti, and R; y=0.33 and 0.15), and $\mathrm{Y_{1-x}Ca_xSrBaCu_{3-y}M_yO_{6+z}}$ (M=Al, Co, Fe, and Ga, y=0, 0.4).[39] These observations indicate that the substitution of $\mathrm{Ca^{2+}}$ for $\mathrm{Y^{3+}}$ in these compounds compensates the loss of the holes and restores the superconductivity.

The T_c of $\mathrm{Y_{1-x-y}Pr_xCa_yBa_2Cu_3O_{7-z}}$ (Ref. 22) could be enhanced by Ca doping and there exists a maximum of T_c ($T_{c,\max}$) for varying Ca concentration y. The T_c vs y curves can be resolved into two parts: (1) the counteracting effects of generation and filling of holes on the $\mathrm{CuO_2}$ sheets by $\mathrm{Ca^{2+}}$ and $\mathrm{Pr^{4+}}$ ions, respectively, and (2) the depairing of superconducting electrons via exchange interaction of mobile holes on the $\mathrm{CuO_2}$ sheets with local Pr magnetic moments. Combining the features of both models, Neumeier *et al.*[22] suggested an empirical polynomial function,

$$T_c = T_{c0} - A(\alpha - \beta x + y)^2 - Bx, \quad (3)$$

where T_{c0} is the maximum obtained value of T_c, $A(\alpha - \beta x + y)^2$ is an empirical term that represents the effect of hole generation by Ca ions and hole filling by Pr ions, $-\alpha$ is an optimal hole concentration, β is the deviation of the effective valence, $\nu(\mathrm{Pr})$, of Pr ions from $+3$ [i.e., $\beta = \nu(\mathrm{Pr}) - 3$], $-Bx$ describes the overall depression of T_c with x due to the pair-breaking mechanism.

In this paper we study the effect of codoping of Pr and Ca on T_c in $\mathrm{R_{1-x-y}Pr_xCa_yBa_2Cu_3O_{7-z}}$ (R=Er, Dy, Gd, Eu, Sm, and Nd), and observe a rare-earth ion-size effect on T_c in these systems. For fixed Pr and Ca concentration, T_c is linearly dependent on rare-earth ion radius r_R^{3+}. We proposed an empirical formula for T_c (r_R^{3+}, x, y) to fit our experimental data.

II. EXPERIMENTAL

Polycrystalline samples $\mathrm{R_{1-x-y}Pr_xCa_yBa_2Cu_3O_{7-z}}$ (R=Er, Dy, Gd, Eu, Sm, and Nd) were prepared by standard solid-state reaction method. Stoichiometry amounts of high-purity R_2O_3, Pr_6O_{11}, $CaCO_3$, $BaCO_3$, and CuO powders were mixed, ground and calcined three times at 900, 910, 920 °C, respectively, for 24 h followed by furnace cooling to room temperature. Each time the powders were ground and mixed before next firing for ensuring the homogeneity of samples. The resultant powders were reground and pressed under the pressure 40 kg/cm^3 into pellets, which were sintered in flowing oxygen at 930 °C for 30 h followed by a slow cooling to 680 °C staying for 8 h, and then slowly

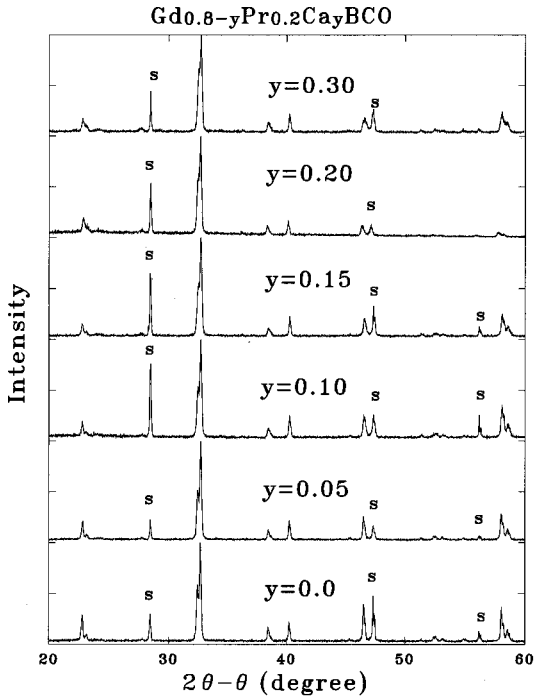

FIG. 1. X-ray powder-diffraction patterns for $Gd_{0.8-y}Pr_{0.2}Ca_yBa_2Cu_3O_{7-z}$ ($y=0-0.3$). Si peaks are labeled by symbol ''s.''

cooled to 450 °C for 30 h before a final cool to room temperature.

The structure of the samples were examined by Rigaku Rotaflex rotating anode x-ray diffractometer using Cu $K\alpha$ radiation with a wavelength = 1.5406 Å. Differential thermal analysis was also carried out in several groups of samples to check the presence of other phases. T_c was determined from electrical resistivity measurement using a low-frequency (37 Hz) four-lead technique. The measuring current is limited to 20 μA. Electrical contacts to the samples were made by silver-paste epoxy. The dc magnetization was measured by a Quantum design superconducting quantum interference device magnetometer.

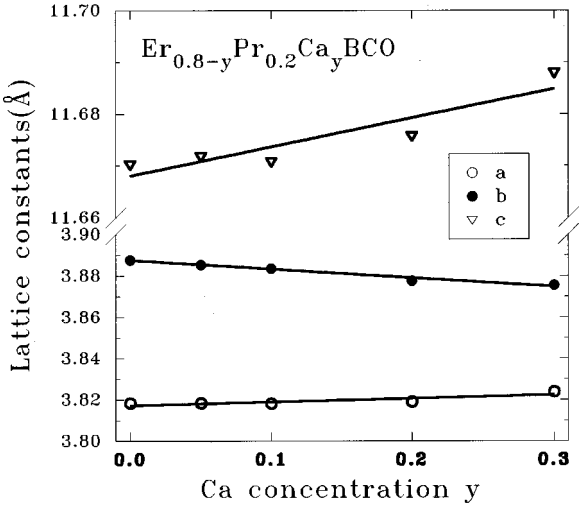

FIG. 2. Lattice constants **a**, **b**, and **c** vs Ca concentration y for $Er_{0.8-y}Pr_{0.2}Ca_yBCO$.

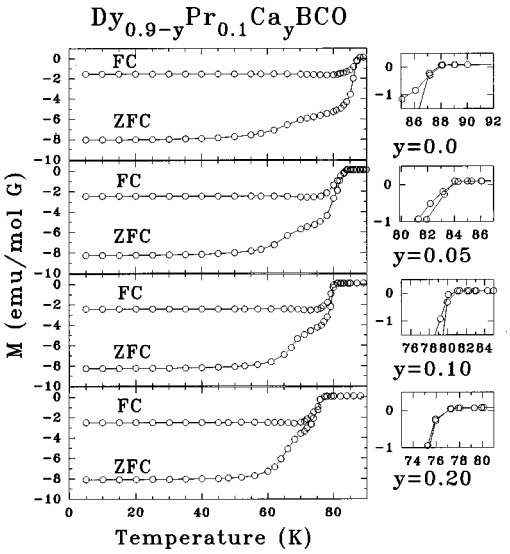

FIG. 3. Temperature dependence of dc molar magnetization (ZFC and FC) for $Dy_{0.9-y}Pr_{0.1}Ca_yBCO$ ($y=0-0.2$). The smaller pictures in the right column show the T_{conset}.

III. RESULTS AND DISCUSSION

X-ray-diffraction patterns at room temperature show that all samples have layered orthorhombic perovskitelike structure and no extra peaks arising from the impurity phases within the experimental errors (<5%). As an example, the x-ray powder-diffraction patterns of $Gd_{0.8-y}Pr_{0.2}Ca_yBa_2Cu_3O_{7-z}$ are shown in Fig. 1. The additional peaks, labeled by symbol ''*s*'', are arising from silicon, added as a standard in order to determine the lattice parameters of our samples. These results indicate Ca doping ($y\leqslant 0.3$) in *R*BCO does not yield impurity phases in bulk material.

The lattice parameters **a**, **b**, and **c** of $Er_{0.8-y}Pr_{0.2}Ca_yBa_2Cu_3C_{7-z}$ are shown in Fig. 2. The *c* axis increases with increasing Ca concentration *y*. It is due to that the radius of Ca ions (99 pm) is much larger than that of Er ions (89

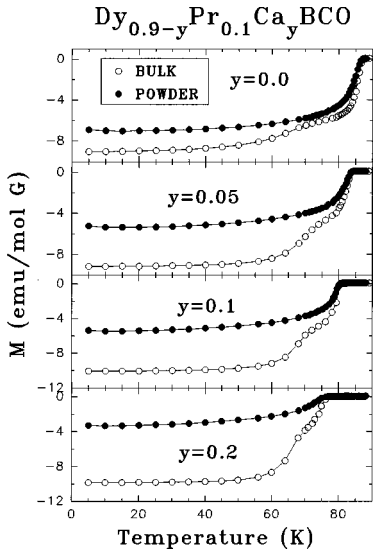

FIG. 4. Temperature dependence of dc molar magnetization (ZFC) for bulk and powder samples of $Dy_{0.9-y}Pr_{0.1}Ca_yBCO$ ($y=0-0.2$).

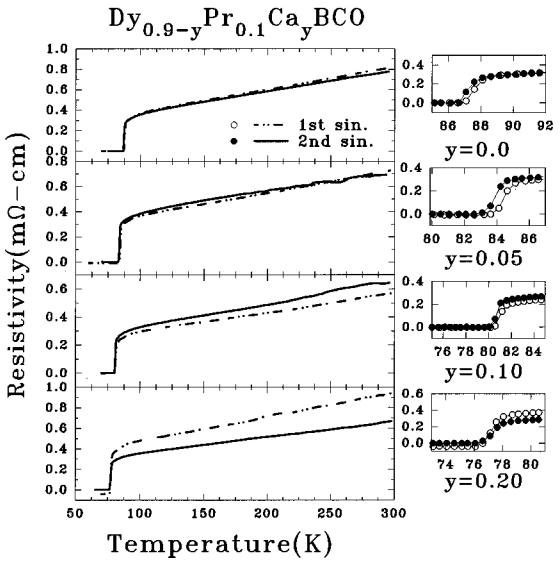

FIG. 5. Temperature dependence of resistivity ρ for $Dy_{0.9-y}Pr_{0.1}Ca_yBCO$ ($y=0-0.2$). The smaller pictures in the right column show the T_{cmid}. Two samples were sintered with the same condition.

pm). This increment is reduced in other $R_{1-x-y}Pr_xCa_yBa_2Cu_3O_{7-z}$ system where the R ion radius is larger. The lattice parameter **b** decreases and **a** increases slightly with increasing Ca concentration y. These behaviors are similar to that reported in the $Y_{1-x}Ca_xBa_2Cu_3O_{7-y}$ system.[42] Yang *et al.*[41] reported that the c axis of $R(Ba_{1-x}Ca_x)Cu_3O_{7-z}$ (R=Y and Pr) decreases abruptly, where Ca ions occupy the Ba site and it is just opposite to the observed result shown in Fig. 2. Therefore, we believe that the Ca ions replace the R site but not the Ba site in our $R_{1-x-y}Pr_xCa_yBa_2Cu_3O_{7-z}$ samples.

It was reported that in fully oxygenated YBCO, Ca doping is accompanied by the loss of oxygen content,[40] but it was also reported that the oxygen content does not change with Ca concentration in the $Y_{1-x-y}Pr_xCa_yBa_2Cu_3O_{7-z}$ system.[22] It suggests that the loss of oxygen content, resulting from Ca doping, can be compensated by Pr doping. On the other hand, in oxygen-deficient YBCO,[42] the length of the c axis increases progressively with decreasing oxygen content. When the R ion radius is comparable to that of Ca ions in our $R_{1-x-y}Pr_xCa_yBa_2Cu_3O_{7-z}$ samples, the c axis does not increase apparently. (For example, in $Eu_{0.8-y}Pr_{0.2}Ca_yBa_2Cu_3O_{7-z}$, $c=11.698$ Å, when $y=0$ and $c=11.707$ Å, when $y=0.2$. $r_{Eu}^{3+}=95$ pm). Therefore, it is reasonable to assume the oxygen content does not vary much in our samples.

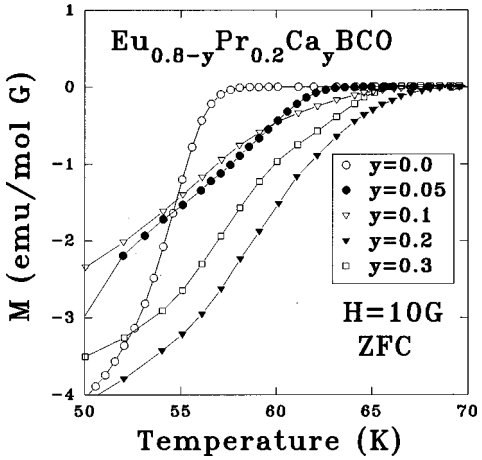

FIG. 7. Temperature dependence of dc molar magnetization (ZFC) for bulk samples of $Eu_{0.8-y}Pr_{0.2}Ca_yBCO$ ($y=0-0.3$).

The temperature dependence of dc molar magnetization $M(T)$ of $R_{1-x-y}Pr_xCa_yBa_2Cu_3O_{7-z}$ was measured both in zero-field cooling (ZFC) and field-cooling (FC) over the temperature range 5–90 K in the magnetic field of 10 G. A typical result for $Dy_{0.9-y}Pr_{0.1}Ca_yBa_2Cu_3O_{7-z}$ is shown in Fig. 3. The $M(T)$ curves demonstrate a superconducting transition with a ''knee'' in ZFC. It could be due to the granular character of the sintered samples. The superconducting transition of sintered pellets could be divided as a two-step process with first the transition of grains and followed by the transition of intergrain barriers or junctions at lower temperatures. The ''knee''disappears when the sample is ground and when the powder dc magnetization measurements are performed as shown in Fig. 4.

Normal-state resistivity $\rho(T)$ was measured in the tem-

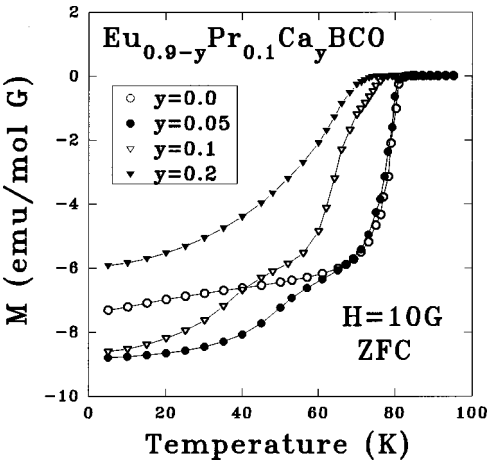

FIG. 6. Temperature dependence of dc molar magnetization (ZFC) for bulk samples of $Eu_{0.9-y}Pr_{0.1}Ca_yBCO$ ($y=0-0.2$).

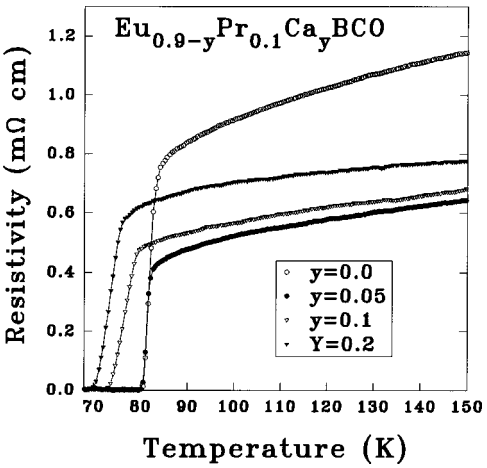

FIG. 8. Temperature dependence of resistivity ρ for $Eu_{0.9-y}Pr_{0.1}Ca_yBCO$ ($y=0-0.2$).

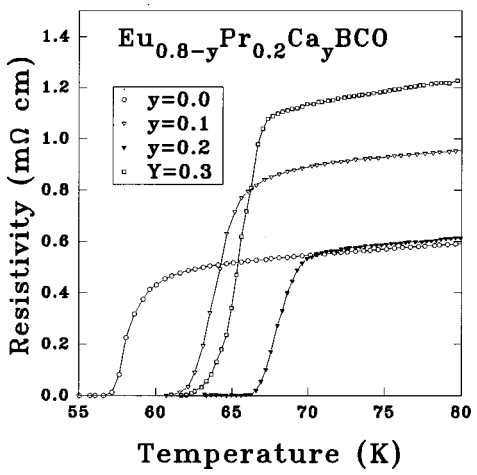

FIG. 9. Temperature dependence of resistivity ρ for $Eu_{0.8-y}Pr_{0.2}Ca_yBCO$ ($y=0-0.3$).

perature range between T_c and 290 K. All samples are ''metallic'' with linear temperature dependence before reaching the superconducting transition temperature. Typical resistivity vs temperature data $\rho(T)$ for $Dy_{0.9-y}Pr_{0.1}Ca_yBa_2Cu_3O_{7-z}$ are shown in Fig. 5. T_c is defined as the temperature at which ρ drops to 50% of its extrapolated normal-state resistivity.

The $M(T)$ and $\rho(T)$ of $Eu_{0.9-y}Pr_{0.1}Ca_yBa_2Cu_3O_{7-z}$ and $Eu_{0.8-y}Pr_{0.2}Ca_yBa_2Cu_3O_{7-z}$ are shown in Figs. 6–9.

Both $M(T)$ and $\rho(T)$ of $Eu_{0.8-y}Pr_{0.2}Ca_yBa_2Cu_3O_{7-z}$ exhibit that T_c is raised by Ca doping before y reaches 0.2 and then decreases with more Ca doping due to the overdoping effect. There is a distinct maximum ($T_{c,\max}$) in T_c vs Ca concentration y. The enhancement of T_c ($\Delta T_{c,\max}=T_{c,\max}-T_{c,y=0}\approx 11$ K at $y=0.2$, $T_{c,y=0}$ is the transition temperature T_c without Ca doping) is much larger than that in

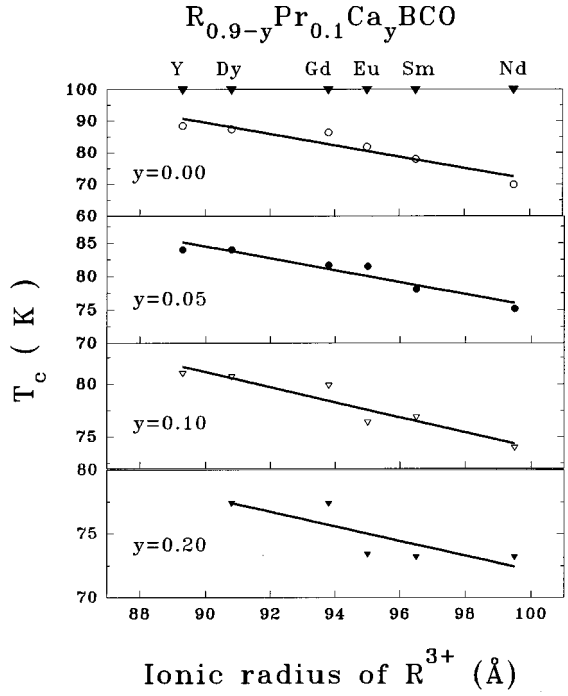

FIG. 10. T_c vs ionic radius of R^{3+} for $R_{0.9-y}Pr_{0.1}Ca_yBCO$ (R = Y, Dy, Gd, Eu, Sm, and Nd; $y=0-0.2$) systems. T_c of $Y_{0.9}Pr_{0.1}Ca_yBCO$ were taken from Ref. 22.

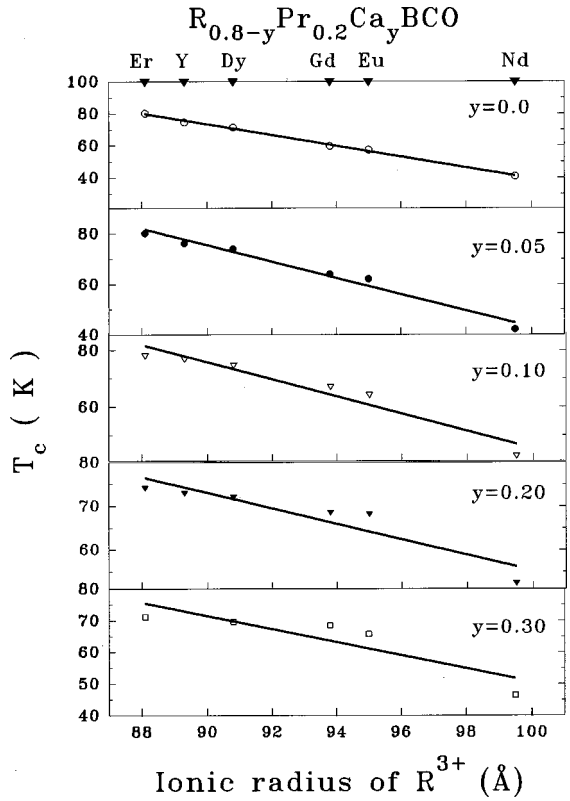

FIG. 11. T_c vs ionic radius of R^{3+} for $R_{0.8-y}Pr_{0.2}Ca_yBCO$ (R = Er, Y, Dy, Gd, Eu, and Nd; $y=0-0.3$) systems. T_c of $Y_{0.8}Pr_{0.2}Ca_yBCO$ were taken from Ref. 22.

$Y_{0.8-y}Pr_{0.2}Ca_yBa_2Cu_3O_{7-z}$,[22] ($\Delta T_{c,\max}\approx 2.5$ K at $y=0.1$). For Pr concentration $x=0.1$, the substitution of 5% Ca does not change T_c substantially and when y is increased to 0.1, T_c is decreased by 5.3 K indicative of $T_{c,\max}$ located in the region $0<y<0.05$.

Superconducting transition temperatures T_c as a function of R ion radius r_R^{3+} for $R_{1-x-y}Pr_xCa_yBa_2Cu_3O_{7-z}$ are shown in Fig. 10 ($x=0.1$) and Fig. 11 ($x=0.2$), which demonstrate that T_c decreases approximately linearly with increasing r_R^{3+}. The solid lines in the figures are the linear fitting. The observed rare-earth ion size effect on T_c in $R_{1-x-y}Pr_xCa_yBa_2Cu_3O_{7-z}$ systems is similar to that in

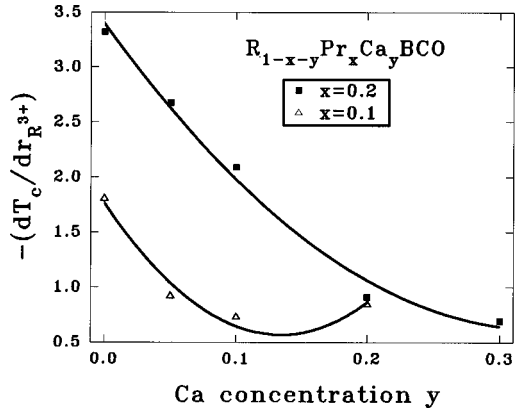

FIG. 12. $-(dT_c/dr_R^{3+})$ vs Ca concentration y for $R_{1-x-y}Pr_xCa_yBCO$. The lines drawn through the data are guides to the eyes.

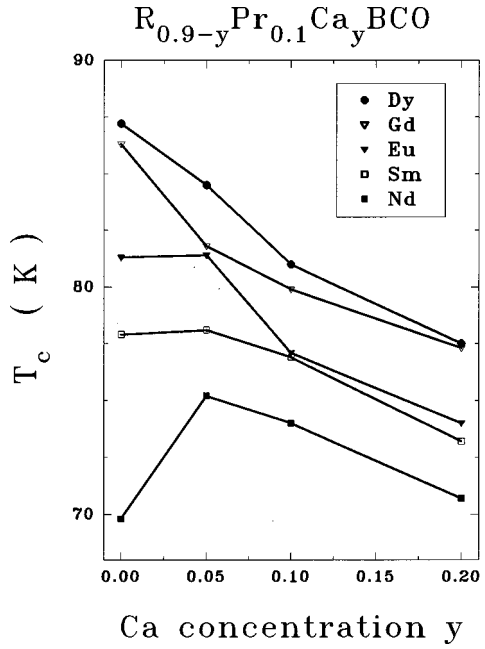

FIG. 13. T_c vs Ca concentration y for $R_{0.9-y}Pr_{0.1}Ca_yBCO$ (R = Dy, Gd, Eu, Sm, and Nd). The lines drawn through the data are guides to the eyes.

$R_{1-x}Pr_xBa_2Cu_3O_{7-z}$ systems in our previous reports.[27–31]

The negative slope of the solid lines in Figs. 10 and 11, $-dT_c/dr_R^{3+}$, are plotted in Fig. 12. For $x=0.2$, the $-dT_c/dr_R^{3+}$ decreases monotonically with increasing Ca concentration y. For $x=0.1$, the $-dT_c/dr_R^{3+}$ decreases with increasing Ca concentration y in the region $0<y<0.1$, but saturates at about $y=0.15$. These results imply that the rare-earth ion size dependence of T_c is weaker in $R_{1-x-y}Pr_xCa_yBa_2Cu_3O_{7-z}$ for increasing Ca concentration y and that the trend of rare-earth ion size effect on T_c for Ca-doped RBCO is opposite to that for Pr-doped RBCO.[27–31]

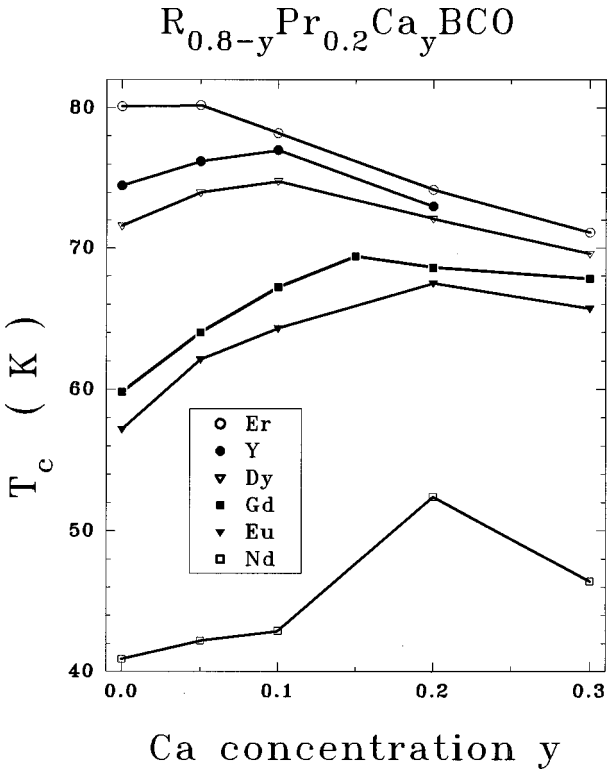

FIG. 14. T_c vs Ca concentration y for $R_{0.8-y}Pr_{0.2}Ca_yBCO$ (R = Er, Y, Dy, Gd, Eu, and Nd). T_c of $Y_{0.8}Pr_{0.2}Ca_yBCO$ were taken from Ref. 22. The lines drawn through the data are guides to the eyes.

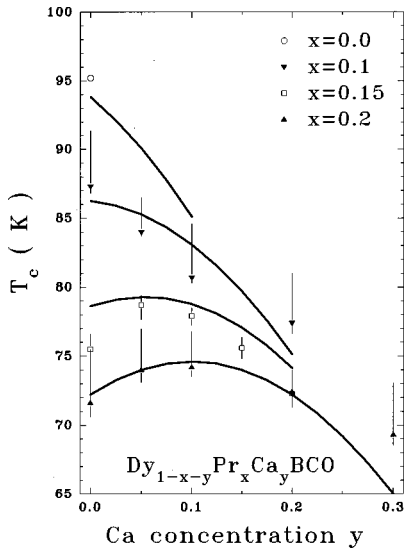

FIG. 15. T_c vs Ca concentration y for $Dy_{1-x-y}Pr_xCa_yBCO$. T_c are obtained from resistivity measurements with the error bars defined by the transition width. The solid lines drawn through the data represent the fitting curves of Eq. (4).

T_c of $R_{1-x-y}Pr_xCa_yBa_2Cu_3O_{7-z}$ for $x=0.1$ and $x=0.2$ as a function of Ca concentration y are shown in Figs. 13 and 14, respectively. In the case of Pr concentration $x=0.1$ (Fig. 13), the monotonic decrease of T_c with increasing Ca concentration y for samples with a smaller R ion (Dy and Gd) implies that the $T_{c,\max}$, possibly, locates in the region $0<y<0.05$. For Pr concentration $x=0.2$ (Fig. 14), a $T_{c,\max}$ is clearly visible in each series. For a sample with a larger R ion radius, $T_{c,\max}$ in T_c vs y curves shifts to higher Ca concentration y, which reveals that a larger number of Ca ions are required to compensate the reduction of the mobile holes. Figure 14 indicates that the enhancement of T_c ($\Delta T_{c,\max}$) becomes larger for sample with a larger R ion radius.

In order to make a quantitative analysis for $T_c(x,y)$, we fit our data using the Eq. (3), $T_c=T_{c0}-A(\alpha-\beta x+y)^2-Bx$.

Typical results of fitting for $Dy_{1-x-y}Pr_xCa_yBa_2Cu_3O_{7-z}$ and $Gd_{1-x-y}Pr_xCa_yBa_2Cu_3O_{7-z}$ are shown in Figs. 15 and 16. The symbols represent the T_c, obtained from resistivity measurements, associated with the vertical bars indicating the transition width. The resultant parameters of fitting for $R_{1-x-y}Pr_xCa_yBa_2Cu_3O_{7-z}$ (R=Y, Dy, Gd, Eu, and Nd) are shown in Table I. Some parameters, for example, A and α, seem scattered with respect to R ion radius. It is inconsistent with the results that $T_c(r_R^{3+},x,y)$ itself depends on the R ion radius linearly for fixed x and y as shown in Figs. 10 and 11. This discrepancy might be due to the fact that Ca ions do not contribute an equal number of holes to CuO_2 planes for samples with different R ion radius.

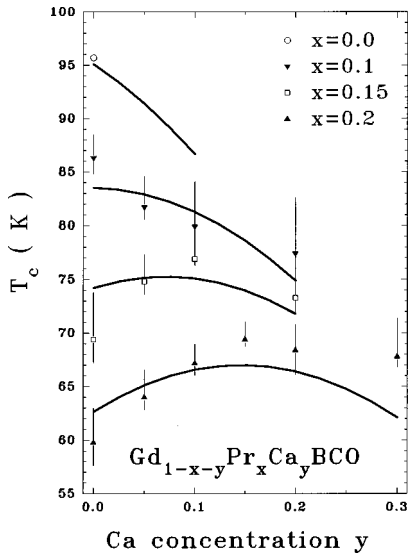

FIG. 16. T_c vs Ca concentration y for $Gd_{1-x-y}Pr_xCa_yBCO$. T_c are obtained from resistivity measurements with the error bars defined by the transition width. The solid lines drawn through the data represent the fitting curves of Eq. (4).

Guan *et al.*[31] reported that the Hall number $\mathbf{n}_H$ (cell^{-1}) of $R_{0.9}Ca_{0.1}Ba_2Cu_3O_{7-z}$ (R=Tm, Ho, Gd, and Nd) increases with decreasing R ion radius. In $Nd_{0.9}Ca_{0.1}Ba_2Cu_3O_{7-z}$ and $Tm_{0.9}Ca_{0.1}Ba_2Cu_3O_{7-z}$ systems, $\mathbf{n}_H$ (cell^{-1}) at 100 K is about 0.5 and 2.0, respectively. For pure RBCO, $\mathbf{n}_H$ at 100 K is about 0.4 in $NdBa_2Cu_3O_{7-z}$ and 0.6 in $YBa_2Cu_3O_{7-z}$.[4,25] It should be noticed that the difference of $\mathbf{n}_H$ between $Nd_{0.9}Ca_{0.1}Ba_2Cu_3O_{7-z}$ and $Tm_{0.9}Ca_{0.1}Ba_2Cu_3O_{7-z}$ is much larger (about 7 times) than that between $NdBa_2Cu_3O_{7-z}$ and $YBa_2Cu_3O_{7-z}$. It suggests that Ca ions contribute much more mobile holes to CuO_2 sheets in $Tm_{0.9}Ca_{0.1}Ba_2Cu_3O_{7-z}$ than in $Nd_{0.9}Ca_{0.1}Ba_2Cu_3O_{7-z}$. On the other hand, the reported $\mathbf{n}_H$ is about 0.3 in $Nd_{0.8}Pr_{0.2}Ba_2Cu_3O_{7-z}$ (Ref. 30) and 0.4 in $Y_{0.8}Pr_{0.2}Ba_2Cu_3O_{7-z}$.[43] The difference of $\mathbf{n}_H$ between them is also as small as that between $NdBa_2Cu_3O_{7-z}$ and $YBa_2Cu_3O_{7-z}$. We suggest that the Eq. (3) should be modified to following form:

$$T_c(x,y)=T_{c0}-A\beta^2(\alpha/\beta-x+y/\beta)^2-Bx, \qquad (4)$$

where $A\beta^2(\alpha/\beta-x+y/\beta)^2$ is equivalent to $A(\alpha-\beta x+y)^2$ in Eq. (3), $-\alpha/\beta$ is an optimal hole concentration, and $1/\beta$ is the number of holes contributed by a Ca ion to CuO_2 planes. The parameters in Eq. (4), T_{c0}, B, β, α/β, and $A\beta^2$, as a function of R ion radius are shown in Fig. 17. Our data

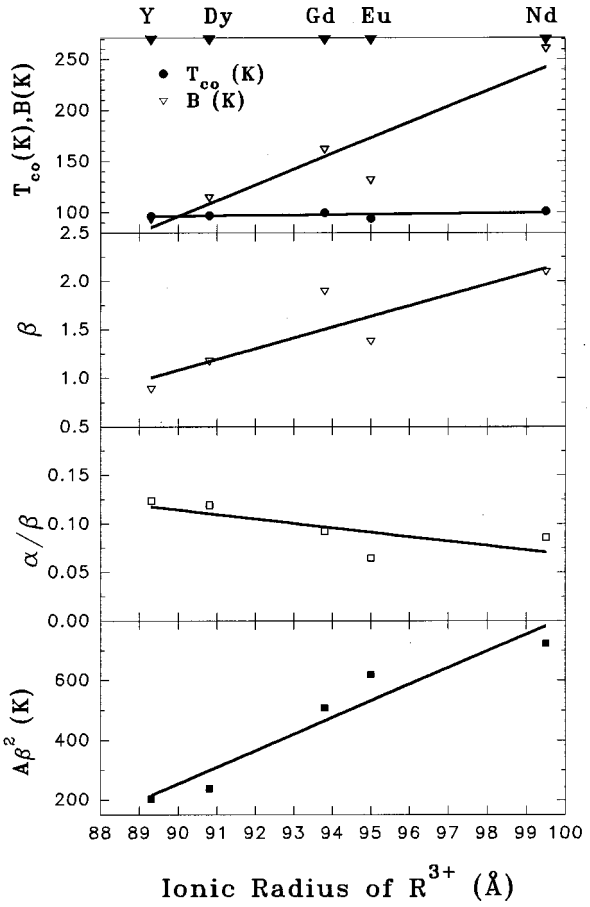

FIG. 17. The fitting parameters of the Eq. (4), T_{c0} (K), B (K), β, α/β, and $A\beta^2$ (K)] vs ionic radius of R^{3+} for $R_{1-x-y}Pr_xCa_yBCO$ (R=Y, DY, Gd, Eu, and Nd) systems: The solid lines represent the linear fitting.

established that all parameters, T_{c0}, $A\beta^2$, B, α/β, and β, depend on the R ion radius linearly.

The parameter B increases with increasing R ion radius, indicating a stronger pair-breaking effect due to Pr doping for a sample with larger R ion radius, which is consistent with the R ion-size effect observed in $R_{1-x}Pr_xBa_2Cu_3O_{7-z}$.[27–31]

T_{c0} increases slightly with increasing R ion radius. This result is in accordance with the earlier results for pure $RBa_2Cu_3O_{7-z}$.[1] α/β is positive and decreases with increasing R ion radius, indicating that the pure and fully oxygenated $RBa_2Cu_3O_{7-z}$ are all in the overdoped region.

β increases with increasing R ion radius, indicating that

TABLE I. The fitting parameters of equation (by the least-squares method): $T_c=T_{c0}-A(\alpha-\beta x+y)-Bx=T_{c0}-A\beta^2(\alpha/\beta-x+y/\beta)-Bx$ for $R_{1-x-y}Pr_xCa_yBa_2Cu_3O_{7-\delta}$.

R	α	β	A (K)	B (K)	T_{c0} (K)	$A\beta^2$	$x_c=\alpha/\beta$
Y	0.11	0.89	256	93.8	96.4	203	0.124
Dy	0.14	1.18	172	115	97.0	238	0.119
Gd	0.175	1.90	141	162	99.6	509	0.092
Eu	0.089	1.38	325	132	94.3	619	0.065
Nd	0.18	2.10	164	261	101	723	0.086

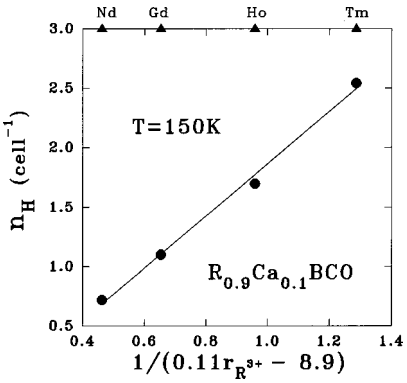

FIG. 18. Hall number $\mathbf{n}_H$ at 150 K vs $1/(0.11r_R^{3+}-8.9)$ for $R_{0.9}Ca_{0.1}BCO$ systems. (R=Tm, Ho, Gd, and Nd).

the number of holes contributed by Ca ions decreases with increasing R ion radius. β could be fitted by a linear relation, $\beta=-8.9+0.11r_R^{3+}$.

Guan *et al.*[31] reported that the Hall number $\mathbf{n}_H$ (cell^{-1}) of $R_{0.9}Ca_{0.1}Ba_2Cu_3O_{7-z}$ (R=Tm, Ho, Gd, and Nd) increases linearly with respect to $(r_R^{3+}-r_{Ca}^{2+})^2$. Especially noteworthy are that $1/\beta$ is the number of holes contributed by a Ca ion to CuO_2 planes and it should be related to mobile holes, $\mathbf{n}_H$. As illustrated in Fig. 18, the measured $\mathbf{n}_H$ (Ref. 31) is, indeed, proportional to $1/(0.11r_R^{3+}-8.9)$. It strongly supports the validity of Eq. (4).

The parameter $A\beta^2$ increases with increasing R ion radius, suggesting a sharper carrier concentration dependence of T_c for sample with larger R ion radius.

Finally, an overall T_c as a function of r_R^{3+}, x, and y in $R_{1-x-y}Pr_xCa_yBa_2Cu_3O_{7-z}$ is proposed. All parameters in Eq. (4), T_{c0}, $A\beta^2$, B, α/β, and β, depend on the R ion radius linearly (see Fig. 17):

$$T_c(r_R^{3+},x,y)=(55+0.46r_R^{3+})-(56r_R^{3+}-4800)[0.47-3.9\times10^{-3}r_R^{3+}-x+y/(0.11r_R^{3+}-8.9)]^2+(17r_R^{3+}-1400)x, \quad \text{for } r_R^{3+}\geqslant 84 \text{ pm.} \quad (5)$$

In conclusion, we observed a rare-earth ion-size effect on T_c in $R_{1-x-y}Pr_xCa_yBa_2Cu_3O_{7-z}$ (R=Er, Dy, Gd, Eu, Sm, and Nd) systems which is similar with that in $R_{1-x}Pr_xBa_2Cu_3O_{7-z}$ systems in our previous reports.[27–31] For fixed Pr and Ca concentration (fixed x and y), T_c is linearly dependent on rare-earth ion radius r_R^{3+}. We proposed an empirical formula for T_c (r_R^{3+},x,y) to fit our experimental data. All fitting parameters in this formula, T_{c0}, B, β, α/β, and $A\beta^2$, are rare-earth ion-size dependent.

ACKNOWLEDGMENTS

The authors wish to acknowledge the assistance of S. R. Sheen and H. F. Lai with the measurements. We also thank D. H. Chen for the analysis of the x-ray data and S. H. Cheng for his useful discussion. This study was supported by National Science Council, R.O.C.

[1] M. B. Maple, Y. Dalichaough, J. M. Ferreira, R. R. Hake, B. W. Lee, J. J. Neumeier, M. S. Torikachvili, K. N. Yang, and H. Zhou, Physica B **148**, 155 (1987), and references therein.

[2] Yunhui Xu and Weiyan Guan, Appl. Phys. Lett. **53**, 334 (1988).

[3] J. K. Liang, X. T. Xu, S. S. Xie, G. H. Rao, X. Y. Shao, and Z. G. Duan, Z. Phys. B **69**, 137 (1987); L. Solderhelm, K. Zhang, D. G. Hinks, M. A. Beno, J. D. Jorgensen, C. U. Serge, and I. K. Schuller, Nature (London) **328**, 6655 (1987).

[4] Y. Dalichaouch, M. S. Torikachvili, E. A. Early, B. W. Lee, C. L. Seaman, K. N. Yang, H. Zhou, and M. B. Maple, Solid State Commun. **65**, 1001 (1988).

[5] A. Matusuda, K. Kinoshita, T. Ishii, H. Shibata, T. Watanabe, and T. Tamada, Phys. Rev. B **38**, 2910 (1988).

[6] J. L. Peng, P. Klavins, R. N. Shelton, H. B. Radousky, P. A. Hahn, and L. Bernardez, Phys. Rev. B **40**, 4517 (1989).

[7] A. P. Goncalves, I. C. Santos, E. B. Lopes, R. T. Henriques, and M. Almeida, Phys. Rev. B **37**, 7476 (1988).

[8] D. W. Cook, R. S. Kwok, R. L. Lichti, T. R. Adams, C. Boekema, W. K. Dawson, A. Kebede, J. Schwegler, J. E. Crow, and T. Mihalisin, Phys. Rev. B **41**, 4801 (1990).

[9] B. Renker, F. Gompf, E. Gering, G. Roth, W. Reichardt, D. Ewert, H. Rietschel, and H. Mutka, Z. Phys. B **71**, 437 (1988).

[10] N. Sanker, V. Sankaranarayanan, L. S. Vaidhyanathan, G. Rangarajan, R. Srinivasan, K. A. Thomas, U. V. Varadaraju, and G. V. Subba Rao, Solid State Commun. **67**, 391 (1988).

[11] U. Neukirch, C. T. Simmons, P. Sladeczac, C. Laubschat, O. Strebel, G. Kaindl, and D. D. Sarma, Europhys. Lett. **5**, 167 (1988).

[12] D. P. Norton, D. H. Lowndes, B. C. Sales, J. D. Budai, B. C. Chakoumakos, and H. R. Kerchner, Phys. Rev. Lett. **66**, 1537 (1991).

[13] R. F. Wood, Phys. Rev. Lett. **66**, 829 (1991), and references therein.

[14] Y. Tokura, J. B. Orrance, T. C. Huang, and A. I. Nazzal, Phys. Rev. B **38**, 7156 (1988); M. W. Shafer, T. Penney, B. L. Olson, R. L. Greene, and R. H. Koch, *ibid.* **39**, 2914 (1989).

[15] J. S. Kang, J. W. Allen, Z. X. Shen, W. P. Willis, J. J. Yeh, W. Lee, M. B. Maple, W. E. Spicer, and I. Laudau, J. Less-Common Met. **148**, 121 (1988).

[16] L. Solderholm and G. L. Goodman, J. Solid State Chem. **81**, 121 (1989).

[17] H. J. Rosen, R. M. Macfarlance, E. M. Engler, V. Y. Lee, and R. D. Jacowitz, Phys. Rev. B **38**, 2460 (1988).

[18] J. Fink, N. Nucker, H. Romberg, M. Alexander, M. B. Maple, J. J. Neumeier, and J. W. Allen, Phys. Rev. B **42**, 4823 (1990).

[19] H.-C. I. Kao, F. C. Yu, and Weiyan Guan, Physica C **292**, 53 (1997).

[20] A. A. Abrikosov and L. P. Gor'kov, Zh. Eksp. Teor. Fiz. **39**, 1781 (1960); Sov. Phys. JETP **12**, 1243 (1961).

[21] C. Jee, A. Kebede, D. Nichols, J. E. Crow, T. Mihalisin, G. H. Myer, I. Perez, R. E. Salomon, and P. Schlottmann, Solid State Commun. **69**, 379 (1989).

[22] J. J. Neumeier, T. Bjfrnholm, M. B. Maple, and I. K. Schuller, Phys. Rev. Lett. **63**, 2516 (1989).
[23] Yunhui Xu and Weiyan Guan, Appl. Phys. Lett. **59**, 2183 (1991); Phys. Lett. A **163**, 104 (1992).
[24] G. Y. Guo and W. M. Temmerman, Phys. Rev. B **41**, 6372 (1990).
[25] M. B. Maple, C. C. Almasan, C. L. Seaman, S. H. Han, K. Yoshiara, M. Buchgeister, L. M. Paulius, B. W. Lee, D. A. Gajewski, R. F. Jardim, C. R. Fincher, Jr., G. B. Blanchet, and R. P. Guertin, J. Supercond. **7**, 97 (1994).
[26] R. Fehrenbacher and T. M. Rice, Phys. Rev. Lett. **70**, 3471 (1993).
[27] Yunhui Xu and Weiyan Guan, Phys. Rev. B **45**, 3176 (1992).
[28] Weiyan Guan, Yunhui Xu, S. R. Sheen, Y. C. Chen, J. Y. T. Wei, H. F. Lai, and M. K. Wu, Phys. Rev. B **49**, 15 993 (1994); Weiyan Guan, Y. C. Chen, J. Y. T. Wei, Y. H. Xu, and M. K. Wu, Physica C **209**, 19 (1993).
[29] Y. Chen, T. S. Lai, M. K. Wu, and Weiyan Guan, J. Appl. Phys. **78**, 5212 (1995).
[30] J. C. Chen, Y. H. Xu, M. K. Wu, and Weiyan Guan, Phys. Rev. B **53**, 5839 (1996).
[31] Weiyan Guan, J. C. Chen, S. H. Cheng, and Y. H. Xu, Phys. Rev. B **54**, 6758 (1996); Weiyan Guan, J. C. Chen, and S. H. Cheng, *ibid.* **54**, 3580 (1996).
[32] Yunhui Xu and Weiyan Guan, Physica C **212**, 119 (1993); Yunhui Xu, Weiyan Guan, Y. F. Chen, S. R. Shen, and M. K. Wu, Phys. Rev. B **50**, 1223 (1994); Yunhui Xu, Weiyan Guan, S. S. Ata-Allah, and Ch. Heiden, Physica C **235-240**, 823 (1994).
[33] D. Khomskii, Physica B **199&200**, 328 (1994); D. Khomskii, J. Supercond. **6**, 69 (1993).
[34] Y. Sun, G. Strasser, W. Seidenbusch, and W. Rauch, Physica C **206**, 291 (1993); Y. Sun, G. Strasser, E. Gornik, and X. Z. Wang, *ibid.* **223**, 14 (1993); T. Watanabe, M. Fujiwara, and N. Suzuki, *ibid.* **252**, 100 (1995).
[35] G. Xiao and N. S. Rebello, Physica C **211**, 433 (1993).
[36] H. Yakabe, J. G. Wen, Y. Shiohara, and N. Koshizuka, Physica C **244**, 256 (1995).
[37] E. Surd, A. Maignan, V. Caignaert, and B. Raveau, Physica C **200**, 43 (1992).
[38] M. G. Smith, J. Chan, and J. B. Goodenough, Physica C **208**, 412 (1993).
[39] R. Suryanarayanan, S. Leelaprute, L. Ouhammou, and A. Das, J. Supercond. **7**, 77 (1994).
[40] B. Fisher, J. Genossar, C. G. Kuper, L. Patlagan, G. M. Reisner, and A. Knizhnik, Phys. Rev. B **47**, 6054 (1993).
[41] H. D. Yang, M. W. Lin, C. H. Luo, H. L. Tsay, and T. F. Young, Physica C **203**, 320 (1992).
[42] R. J. Cava, B. Batlogg, S. A. Sunshine, T. Siegrist, R. M. Fleming, K. Rabe, L. F. Schneemeyer, O. W. Murphy, R. B. van Dover, P. K. Gallagher, S. H. Glarum, S. Nakahara, R. C. Farrow, J. J. Krajewski, S. M. Zahurak, J. V. Waszczak, J. H. Marshall, P. Marsh, L. W. Rupp, Jr., W. F. Peck, and E. A. Rietman, Physica C **153-155**, 560 (1988).
[43] Wu Jiang, J. L. Peng, S. J. Hagen, and R. L. Green, Phys. Rev. B **46**, 8694 (1992).